Identification of cardiac oxidoreductase(s) involved in the metabolism of the lipid peroxidation-derived aldehyde-4-hydroxynonenal

Sanjay SRIVASTAVA*, Animesh CHANDRA*, Naseem H. ANSARI*, Satish K. SRIVASTAVA*[1] and Aruni BHATNAGAR*†

*Department of Human Biological Chemistry and Genetics, University of Texas Medical Branch, Galveston, Texas 77555-1067, U.S.A., and †Department of Physiology and Biophysics, University of Texas Medical Branch, Galveston, Texas 77555-1067, U.S.A.

The aim of this study was to identify the cardiac oxidoreductases involved in the metabolism of 4-hydroxy-2-*trans*-nonenal (HNE), an α,β unsaturated aldehyde generated during the peroxidation of $\omega-6$ polyunsaturated fatty acids. In homogenates of bovine, human and rat ventricles the primary pyridine coenzyme-linked metabolism of HNE was associated with NADPH oxidation. The NADPH-dependent enzyme catalysing HNE reduction was purified to homogeneity from bovine heart. The purified enzyme displayed kinetic and immunological properties identical with the polyol pathway enzyme aldose reductase (AR), and catalysed the reduction of HNE to its alcohol 1,4-dihydroxynonene (DHN), with a K_m of 7 ± 2 μM. In the presence of NADP the enzyme did not catalyse the oxidation of DHN. During catalysis, HNE did not cause inactivation of AR. Nevertheless when the apoenzyme was incubated with HNE a dissociable complex was formed between the enzyme and HNE, followed by irreversible loss of activity. Inactivation of the enzyme by HNE was prevented by NADP. Partial modification of the enzyme with HNE led to a 17-fold increase in the $K^{\mathrm{HNE}}{}_{\mathrm{m}}$ and $K^{\mathrm{glyceraldehyde}}{}_{\mathrm{m}}$, and the HNE-modified enzyme had a 500-fold higher IC_{50} for sorbinil than for the reduced enzyme, whereas the IC_{50} for tolrestat increased 25-fold. Incubation of the enzyme with radiolabelled HNE resulted in the incorporation of 2 mol of the aldehyde per mol of the enzyme. Sequence analysis of the radiolabelled peptides revealed modification of Cys-298 and Cys-187. The amino acid sequence of the HNE-modified peptides confirmed that the HNE-reducing cardiac enzyme is AR and not a related protein such as the fibroblast-growth-factor-regulated protein FR-1 or the mouse vas deferens protein MVDP. These results indicate that AR represents the only major oxidoreductase in the heart capable of utilizing HNE. The high affinity of the enzyme for HNE, the lack of inactivation during catalysis, and the lack of significant alcohol dehydrogenase activity of the protein suggests that AR-mediated catalysis of HNE is unlikely to be limited by substrate/product inhibition. Thus AR might constitute an antioxidative enzyme involved in myocardial protection against endogenous and exogenous cytotoxic aldehydes and against oxidative stress.

INTRODUCTION

Increasing evidence suggests that free radicals have a critical role in modulating cellular processes and, if unquenched, lead to necrotic or apoptotic cell death [1]. Several disease and toxicological states as well as the degenerative processes of senescence are thought to be directly or indirectly due to the perturbation of redox state and oxidative stress. Nevertheless the mechanisms by which free radicals affect cellular processes, and/or mediate overt toxicity, are poorly understood and are at present under intense investigation. In the cellular environment, most free radicals are transiently produced and cause mainly local or site-specific alterations. It has been suggested that the pronounced effects of free radicals reactions might be in part due to their propensity to generate cytotoxic products [2]. Such metastable products can diffuse to sites distal from their origin and mediate and extend the initially local injury. In this regard the aldehydes such as 4-hydroxyalkenals, generated from lipid peroxidative reactions, have received most attention, particularly because of the high intracellular concentrations in which they are produced and the marked cytotoxic effects that they display [2]. Several pathological states associated with oxidative stress lead to the accumulation of these aldehydes. The heart seems to be particularly vulnerable to unsaturated aldehydes generated by lipid peroxidation. Cardiac dysfunction and injury due to ischaemia-reperfusion [3], cardiopulmonary bypass [4] and anti-cancer drugs [5] have been shown to be accompanied by elevated levels of hydoxyalkenals. Moreover, high levels of 4-hydroxy-2-*trans*-nonenal (HNE)-modified proteins, including HNE adducts with low-density lipoprotein, have been detected in atherosclerotic plaques [2], and thus free HNE released from oxidized low-density lipoprotein could, in part, contribute to cardiac injury caused by atherosclerosis. However, to assess the contribution of these aldehydes to oxidative stress and to evaluate their proposed role as toxic second messengers it is essential to identify the biochemical pathways responsible for their metabolism and detoxification.

In contrast with well-studied tissues such as liver, little is known of the enzymic routes for the metabolism of hydroxyalkenals in the heart, except that the capacity of the heart to metabolize these aldehydes is low (approximately one-tenth of that of the liver) [2] and that glutathione conjugation catalysed by glutathione S-transferases represents one specific mode of metabolism [6]. However, other subsidiary enzymes involved in the detoxification of these aldehydes might also be present in the heart, particularly the pyridine coenzyme-linked oxidoreductases, which represent a significant route of aldehyde metabolism in other tissues [2,6]. The intent of this work was to identify the

Abbreviations used: AR, aldose reductase; DHN, 1,4-dihydroxynonene; DTT, dithiothreitol; FR-1, fibroblast growth factor inducible protein 1; HNE, 4-hydroxy-2-*trans*-nonenal; IAA, iodoacetic acid; TFA, trifluoroacetic acid.

[1] To whom correspondence should be addressed.

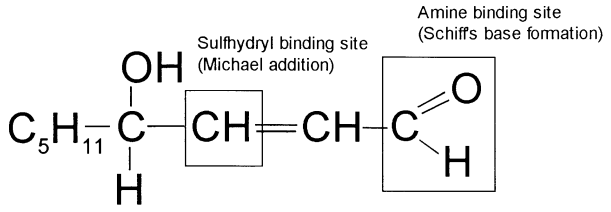

Figure 1 Chemical structure of HNE

The electron-deficient C-3 and the functional aldehyde groups are boxed to show the sites of formation of the Michael adducts and Schiff bases respectively.

pyridine coenzyme-linked enzymes involved in oxidation/-reduction of hydroxyalkenals in heart. For our experiments we used the prototype aldehyde HNE (Figure 1), which is produced by the β-scission of alkoxyl radicals generated during the peroxidation of $\omega-6$ polyunsaturated fatty acids such as arachidonic, linolenic and linoleic acids [2]. The heart is particularly rich in such polyunsaturated fatty acids [7]. HNE is one of the most reactive and cytotoxic aldehydes generated by lipid peroxidation and constitutes up to 95% of the total unsaturated aldehydes produced [8]; exposure of isolated cardiac myocytes to HNE causes metabolic inhibition and leads to pronounced pro-arrhythmic changes [9]. The results of the present study show that the polyol pathway enzyme aldose reductase (AR) represents the major myocardial route of pyridine coenzyme-linked metabolism of HNE. Therefore we propose that AR might be an important component of cardiac defence against aldehyde toxicity in particular and oxidative stress in general.

MATERIALS AND METHODS

Materials

Bovine hearts were obtained from the local abattoir; rat hearts were isolated from male Sprague–Dawley rats weighing 200–260 g. Human hearts were obtained within 6–8 h of death and kept frozen until use. Sephadex G-100, Reactive Blue, NADPH, $NADP^+$, D,L-glyceraldehyde, iodoacetate (IAA) and D,L-dithiothreitol (DTT) were purchased from Sigma Chemical Co. (St. Louis, MO, U.S.A.). PBE-94 and Polybuffer 74 were purchased from Pharmacia Fine Chemicals (Uppsala, Sweden). DEAE-cellulose (DE-52) was obtained from Whatman Co. (Maidstone, Kent, U.K.). Sorbinil [CP-45 643; d6-fluoro-*spiro*(chroman-4,4′-imidazolidine)-2′,5′-dione] and tolrestat {Ay-27773; *N*-methyl-*N*-[(5-trifluoromethyl-6-methoxy-1-napthalenyl)-thiomethyl] glycine} were gifts from Pfizer and Ayrest respectively. All the other reagents were of the highest purity available.

Chemical syntheses

The HNE was synthesized as its dimethyl acetal starting from dimethyl acetal of fumaraldehyde [10]. For the synthesis of [4-^{3}H]HNE the dimethyl acetal of HNE was oxidized to the 4-keto derivative with polymer-supported chromic acid as an oxidizing agent. The ketone was reduced to the dimethyl acetal of HNE by using tritiated $NaBH_4$, and [4-^{3}H]HNE obtained by acid hydrolysis was purified by HPLC. The [4-^{3}H]HNE thus synthesized had a specific radioactivity of 175 mCi/mmol [10]. 1,4-Dihydroxynonene (DHN) was synthesized by $NaBH_4$ reduction of HNE. To a solution of HNE in water a 4-fold molar excess of $NaBH_4$ was added, and the mixture was stirred for 60 min at room temperature. HCl (0.1 M) was then added dropwise to the reaction mixture to bring the pH to 2.0. The mixture was then left in acidic conditions for 30 min (to decompose unreacted $NaBH_4$) and was extracted three times with dichloromethane and purified by HPLC with the system described below.

HPLC purification

Synthesized HNE and DHN were purified by HPLC with a Rainin $ODS_{c\text{-}18}$ column equilibrated with 0.1% trifluoroacetic acid (TFA) at a flow rate of 1 ml/min. The compounds were eluted with a gradient consisting of solvent A (0.1% aqueous TFA) and solvent B [0.1% TFA in 60% (v/v) acetonitrile] at a flow rate of 1 ml/min. The gradient was established such that solvent B reached 16.6% in 20 min and 41.5% in 35 min, and was then held at 41.5% for an additional 30 min, after which solvent B was increased such that it reached 100% in 75 min and was held at this value for an additional 20 min. In this system DHN and HNE eluted at retention times of 53 and 64 min respectively. The identity and the purity of HNE and DHN were established by NMR.

Enzyme purification and assay

All operations during the purification of the enzyme were performed at 0–4 °C. Frozen bovine hearts (2400 g) were thawed and the larger blood vessels were removed. The heart tissue was cut into small pieces and homogenized in buffer A (10 mM phosphate, pH 7.0, containing 5 mM 2-mercaptoethanol) to make a 25% (w/v) homogenate and centrifuged at 10000 ***g*** for 1 h. For the determination of HNE reduction and oxidation, the homogenate was reduced by incubation with 0.1 M DTT for 60 min at 37 °C. Excess DTT was removed by a Sephadex G-25 M PD-10 column equilibrated with nitrogen-saturated 0.1 M potassium phosphate, pH 7.0.

For enzyme purification, solid $(NH_4)_2SO_4$ was added to bring the final concentration to 30% (w/v). The 10000 ***g*** supernatant was brought to 75% (w/v) $(NH_4)_2SO_4$ and the suspension was left at 4 °C for 20 h and then centrifuged at 10000 ***g*** for 60 min. The sediment was suspended in buffer A, dialysed against the same buffer and applied to a DE-52 column (2.5 cm × 70 cm), pre-equilibrated with buffer A, at a flow rate of 30 ml/h. After the column had been washed with 1 litre of buffer A, the adsorbed proteins were eluted with a 2 litre gradient of 0–0.2 M NaCl in buffer A and 10 ml fractions were collected. The enzyme activity in the unadsorbed, washed and eluted fractions was measured as described below. The fractions containing the enzyme activity were pooled, dialysed against 20 litres of buffer B (25 mM imidazole buffer, pH 7.0, containing 5 mM 2-mercaptoethanol) and subjected to chromatofocusing. The enzyme fractions were applied to polybuffer PBE-94 exchanger column (1.5 cm × 15 cm), pre-equilibrated with buffer B, at a rate of 30 ml/h. Elution was performed with polybuffer 74, pH 4.0, diluted 1:8. The fractions (1.0 ml) were monitored for enzyme activity and pH. The enzymically active fractions were pooled, dialysed against buffer A and applied to Reactive Blue CL 6B affinity columns at a flow rate of 10 ml/h and eluted with 0.5 mM NADPH after a wash with 50 ml of the buffer. Enzymically active fractions were pooled and applied to a Sephadex G-100 column (2.5 cm × 100 cm), pre-equilibrated with 50 mM phosphate, at a flow rate of 20 ml/h. Fractions from the Sephadex column were collected and assayed for enzyme activity. The enzymically active fractions were pooled and stored at 4 °C until further use.

The enzyme activity was monitored with 10 mM D,L-glyceraldehyde and 100 μM NADPH in 0.05 mM potassium phosphate, pH 6.0, containing 0.4 M Li_2SO_4 on a Gilford response

spectrophotometer at 340 nm. One unit of enzyme activity is defined as 1 μmol of NADPH oxidized/min per ml. Homogeneity of the enzyme was established by the presence of a single protein band on 2-mercaptoethanol/SDS/PAGE. For Western blotting analysis the enzyme was transblotted [11] and stained with antibodies (diluted 1:500) raised against homogenous human placental AR as described previously [12].

Enzyme modification by IAA and HNE

The reduced enzyme was incubated either with 1.0 mM IAA in 0.1 M Tris/HCl, pH 8.0, or with 0.1 mM HNE in 0.1 mM phosphate, pH 7.0, for 1 h at 37 °C; aliquots were removed at intervals to determine the enzyme activity at 37 °C by using 1.0 mM HNE as substrate. In some experiments, immediately after the incubation, the excess IAA/HNE was removed by passing through a TSK_{3000} gel-filtration column or by filtration through a Sephadex G-25 column. The rate constant for inactivation was obtained by fitting the following equation to the data:

$$y = ae^{-t/\tau} \quad (1)$$

where y is the enzyme activity remaining at time t, a is the pre-exponential term or the intercept and τ is the time constant for inactivation. Data for concentration dependence of the inactivation were analysed with a hyperbolic binding equation:

$$y = I_{max}x/(k+x) \quad (2)$$

where y is the intercept (a) or the observed rate constant k_{obs} ($= 1/\tau$) determined from eqn. (1), I_{max} is the maximal inactivation observed and k is the concentration of HNE required for half-maximal change in the intercept or k_{obs}. Data for $NADP^+$ protection against inactivation were obtained by measuring the rate of inactivation at a given concentration of HNE with various concentrations of $NADP^+$. Because in the presence of $NADP^+$ no initial loss of activity was observed, the data were analysed with the Weibull function:

$$y = \exp(-\lambda t)^{\gamma} \quad (3)$$

where γ and λ are the scale and shape factors respectively. The $t_{\frac{1}{2}}$ for inactivation at various different concentrations of $NADP^+$ was calculated from:

$$t_{\frac{1}{2}} = [\Gamma(1+1/\gamma)]/\lambda \quad (4)$$

where $\Gamma(\gamma)$ is the gamma function. The apparent rate constants for inactivation were calculated from the $t_{\frac{1}{2}}$. Data were then plotted as the ratio of the inactivation rate in the absence of $NADP^+$ to that in the presence of different concentrations of $NADP^+$ against $NADP^+$ concentration. The slope of this plot is the reciprocal of the dissociation constant for $NADP^+$ [13]. All non-linear curve fittings were performed using NFIT (Island Products, Galveston, TX, U.S.A.). Best fits to the data were chosen on the basis of the standard error of the fitted parameter and the lowest value of σ, which is defined as the sum of squares of the residuals divided by the degrees of freedom. Data are presented as means ± S.E.M.

Determination of HNE-binding site

Reduced enzyme (0.47 mg; 13 nmol), was incubated with [4-^{3}H]HNE (2×10^6 c.p.m.) in 100 mM phosphate, pH 7.0, at 37 °C for 1 h. Unlabelled HNE (130 nmol; 10-fold molar excess), was added to the enzyme solution and incubated for an additional 1 h at 37 °C. The incubation was continued for 24 h at 4 °C, after which all unbound radioactivity was removed by ultrafiltration with an Amicon-10 microconcentrator (cut-off molecular mass 10 kDa). Solid urea was then added to the mixture to a final concentration of 6 M, and the enzyme was incubated for 1 h followed by extensive dialysis against 0.5 M *N*-ethylmorpholine/acetate buffer, pH 8.0. The dialysed enzyme was digested by adding trypsin to a ratio of 1:100 (w/w) and the mixture was incubated at 37 °C. After 3 h another aliquot of trypsin in the ratio 1:50 (w/w) was added and the digestion continued for a further 4 h. Digestion was terminated by freezing at −20 °C.

The enzyme digest was subjected to HPLC on a reverse-phase ODS C_{18} column (0.46 cm × 25 cm), pre-equilibrated with 0.1% aqueous TFA. Peptides were eluted with a linear gradient of 0–60% (v/v) acetonitrile containing 0.1% TFA at a flow rate of 1 ml/min for 60 min, monitored at 230 nm with a Beckman Gold System 406. The eluted fractions were collected and assayed for radioactivity. The radioactive peaks were pooled separately and subjected to a second HPLC on a C_{18} column, pre-equilibrated with 15% (v/v) acetonitrile containing 0.1% TFA. Peptides were eluted by a 15–45% (v/v) acetonitrile gradient in 40 min at a flow rate of 1 ml/min; 0.5 ml fractions were collected. Fractions of each of the radioactive peaks were pooled and used for amino acid sequence analysis with a gas-phase sequencer (Applied Biosystems 475A protein sequencer). The amino acid from each cycle of Edman degradation was collected for radioactivity determination.

RESULTS

HNE metabolism in cardiac homogenates

Pyridine coenzyme-linked reduction/oxidation of HNE was determined in cardiac homogenates by using 0.1 mM NADPH, $NADP^+$, NADH or NAD^+. As shown in Table 1, the major coenzyme-linked oxidation/reduction of HNE in bovine and human hearts was associated with the oxidation of NADPH,

Table 1 Pyridine coenzyme-linked aldehyde metabolism in bovine heart homogenates

Cardiac homogenates were prepared as described in the Materials and methods section. The quantities of protein used for assay of rat, human and bovine heart enzymes were 87, 420 and 450 μg respectively. The assay buffer consisted of 0.1 M potassium phosphate, pH 7.0, or 0.05 M potassium phosphate/0.4 M Li_2SO_4, pH 6.0. The concentration of each coenzyme used was 0.1 mM, and the HNE concentration was 0.2 mM. The values are expressed as nmol of NAD(P)(H) reduced or oxidized/min per mg of protein at 37 °C. Abbreviation: n.d., not detectable.

		Enzyme activity (nmol/min per mg)			
		D,L-Glyceraldehyde (10 mM)		HNE (0.2 mM)	
Coenzyme	pH ...	7.0	6.0	7.0	6.0
Bovine heart					
NAD^+		2.1	1.1	1.1	1.1
$NADP^+$		3.2	0.3	1.4	1.4
NADH		1.1	0.7	0.7	0.7
NADPH		3.5	7.5	6.4	7.5
Rat heart					
NAD^+		1.8	1.8	5.5	n.d.
$NADP^+$		5.5	5.5	7.4	3.7
NADH		14.8	1.8	18.5	3.7
NADPH		16.6	42.5	35.1	53.6
Human heart					
NAD^+		n.d.	n.d.	n.d.	n.d.
$NADP^+$		1.1	n.d.	0.8	n.d.
NADH		0.4	n.d.	0.4	n.d.
NADPH		7.6	1.9	3.4	5.0

Table 2 Steady-state kinetic parameters of bovine heart AR

All kinetic parameters were determined at 37 °C in 50 mM potassium phosphate, pH 6.0, containing 0.4 M Li_2SO_4. For the determination of $K^{D,L\text{-glyceraldehyde}}{}_m$ and $K^{HNE}{}_m$ the fixed concentration of NADPH was 0.1 mM and for the determination of $K^{NADPH}{}_m$ the fixed concentration of D,L-glyceraldehyde was 10 mM. All assays were performed with argon-purged buffers and substrates. Reduced enzyme was generated by the reduction of the stored enzyme with 0.1 M DTT for 60 min at 37 °C followed by the removal of excess DTT by gel filtration. The carboxymethylated and the HNE-modified enzymes were generated by incubating the reduced (DTT-free) enzyme with either 1.0 mM IAA or 0.1 mM HNE for 60 min at 37 °C; the reaction was stopped by dilution and rapid gel filtration. Procedural details are described in the Materials and methods section. Data are means ± S.E.M. ($n = 3$).

	K_m (μM)			k_{cat} (min^{-1})	
	NADPH	D,L-Glyceraldehyde	HNE	D,L-Glyceraldehyde/NADPH	HNE/NADPH
Reduced enzyme	15 ± 4	37 ± 7	7 ± 2	27.7	24.7
Carboxymethylated enzyme	40 ± 5	207 ± 31	232 ± 44	17.17	16.8
HNE-modified enzyme	45 ± 7	632 ± 72	121 ± 18	12.5	17.2

with little or no activity due to NAD^+, $NADP^+$ or NADH. In rat heart, low but significant NADH-catalysed reduction of glyceraldehyde and HNE was also observed at pH 7.0. No non-enzymic reaction between HNE and NAD(P)(H) was observed. The NADPH-catalysed reduction of HNE was significantly higher than that associated with other pyridine coenzymes both in pH 7.0, and more so in pH 6.0, buffer containing 0.4 M Li_2SO_4. Furthermore the rate of NADPH-mediated reduction of HNE was similar to the rate of reduction of D,L-glyceraldehyde. In bovine heart homogenates, the $K^{HNE}{}_m$ for the NADPH-linked reduction was 9.5 ± 1.7 μM. From these data we conclude that the NADPH-dependent reduction is the major pyridine coenzyme-linked pathway of HNE metabolism in the heart. To investigate this catalytic activity further, the NADPH-dependent HNE-reducing enzyme was purified to homogeneity.

As described in the Materials and methods section, the first step in the purification protocol was DE-52 column chromatography. The elution profile from the DE-52 column showed a single peak of the NADPH-dependent glyceraldehyde-reducing activity (results not shown). Samples corresponding to this peak were pooled and the NADPH-dependent enzyme was further purified. On chromatofocusing the isoelectric pH of the enzyme corresponded to a pH of 5.64, and on Sephadex gel filtration the enzyme activity eluted as a single peak corresponding to a molecular mass of 34–36 kDa. The purified enzyme migrated as a single band on SDS/PAGE, corresponding to a molecular mass of 36 kDa, which cross-reacted with the antibodies prepared against human placenta AR (results not shown).

Steady-state kinetic parameters of cardiac AR

The steady-state kinetic parameters of the purified enzyme are summarized in Table 2. The K_m and the k_{cat} values of the enzyme ('reduced enzyme') for NADPH and D,L-glyceraldehyde are similar to those reported for AR purified from other tissues [14]. The enzyme displayed a high affinity for HNE ($K_m = 7$ μM) and the catalytic rate of the enzyme with HNE was comparable to that for the reduction of D,L-glyceraldehyde. In initial velocity plots, no significant substrate inhibition was observed (results not shown). Moreover, the progress curves of enzyme activity did not display deviation from linearity ($R^2 = 0.960$–0.999) when HNE was varied from 5 to 100 μM (at a saturating concentration of NADPH, 0.2 mM), indicating that HNE does not cause inactivation of the enzyme during catalysis. Also, no reduction of $NADP^+$ was observed on incubation with the enzyme (0.1 unit) and 1 mM DHN for up to 10 min at 37 °C.

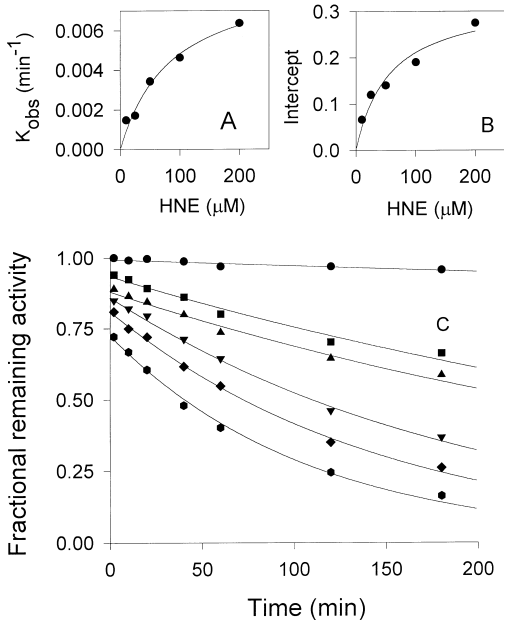

Figure 2 Inactivation of bovine heart AR by HNE

The purified enzyme was reduced with 0.1 M DTT; excess DTT was removed. The reduced enzyme was incubated in nitrogen-purged 0.1 M potassium phosphate, pH 7.0, at 37 °C, without (●) or with 10 μM (■), 20 μM (▲), 50 μM (▼), 100 μM (◆) or 200 μM (⬢) HNE. After the indicated intervals, aliquots of the incubation mixture were withdrawn and the enzyme activity was determined with HNE (1.0 mM) as the substrate. (**C**) Time-dependent changes in the enzyme activity on incubation with the indicated concentrations of HNE. Results are shown as discrete points and the curves are best fits of a monoexponential equation to the data. (**A**, **B**) Dependence of the observed rate of inactivation (k_{obs}) (**A**) and the intercept of the inactivation curves on HNE concentration (**B**). The curves are best fits of a hyperbolic function to the data.

Inactivation of AR by HNE

In contrast to its behaviour as a substrate in the presence of NADPH, HNE caused inhibition of the apoenzyme. Incubation of the enzyme with HNE (0.01–0.2 mM) caused a time- and concentration-dependent inactivation. Approximately 50% of the initial activity was lost when the enzyme was exposed to 0.1 mM HNE at pH 7.0 and 37 °C for 60 min (Figure 2). The rate of loss in enzyme activity exhibited biexponential kinetics. The initial rate of inactivation was too fast to be resolved by steady-state kinetic measurements; however, the fast phase of

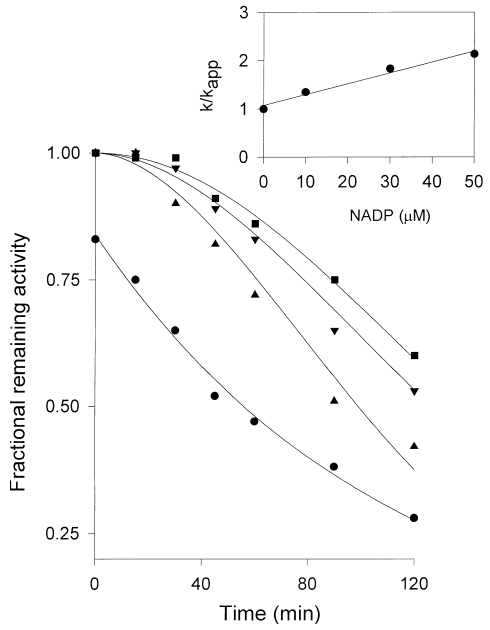

Figure 3 Protection of AR against HNE-induced inactivation by NADP$^+$

The enzyme (0.6 mg/ml) was incubated in nitrogen-purged 0.1 M potassium phosphate, pH 7.0, for 60 min with 100 μM HNE (●) or 1 mM HNE containing 10 (▲), 30 (▼) or 50 (■) μM NADP$^+$, and assayed with 100 μM HNE and NADPH after the indicated intervals. The points are experimental values; the solid curves are theoretical fits of the data to eqn. (1) for inactivation in the presence of HNE and eqn. (3) for HNE and NADP$^+$, with the fitted parameters. Inset: plot of k/k_{app} against NADP$^+$ concentration. The K_i for E·NADP$^+$ obtained from the slope is 41.7 ± 2.7 μM.

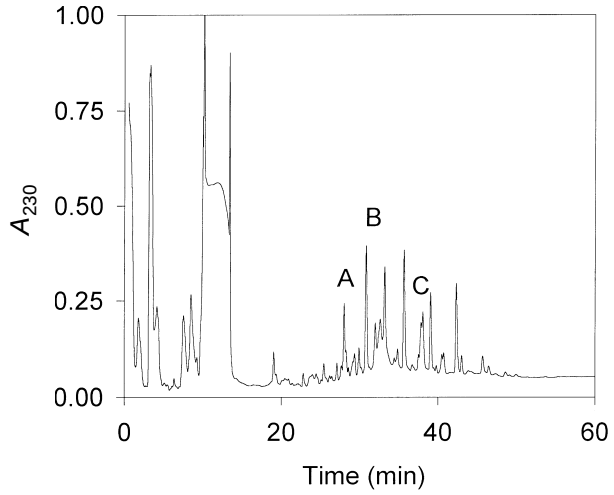

Figure 4 Reverse-phase HPLC of the trypsin digest of [^{3}H]HNE-modified AR

The elution profile shows three major radioactive peaks (labelled A, B and C) at 28.9, 33.3 and 39.4 min, which were eluted with a gradient of 0–60% (v/v) acetonitrile containing 0.1% TFA. Peak fractions containing radioactivity were pooled separately and subjected again to HPLC. The amino acid sequence of the respective peptides, as determined by gas-phase amino acid sequencing, were: peak A, IAENFQVFDFELDKEDMNTLLSYNRWRAC^{298}; peak B, YKPAVNQIEC^{187}HPHYTQEK; peak C, YKPAVNQIEC^{187}.

inactivation was followed by a slow monoexponential inactivation (Figure 2C). The values of the observed rate of inactivation of the enzyme and the intercept of the slow component exhibited a hyperbolic dependence on the concentration of HNE (Figures 2A and 2B), indicating that a significant amount of dissociable complex is formed between the enzyme and HNE before the formation of the inactivated enzyme–HNE complex.

To investigate the mechanism of HNE inactivation further, the effect of NADP$^+$ was studied. Although incubation with HNE led to a monoexponential inactivation, in the presence of NADP$^+$ no inactivation was observed during the initial phase of incubation, for up to 40 min. Prolonged incubation led to an exponential decrease in the catalytic activity of the enzyme (Figure 3). This behaviour was well described by the Weibull function. The rate constants for inactivation in the presence of 0, 10, 30 and 50 μM NADP$^+$ were: $(9.25 \pm 0.4) \times 10^3$, $(6.4 \pm 0.4) \times 10^3$, $(5.0 \pm 0.6) \times 10^3$ and $(4.4 \pm 0.4) \times 10^3$ min^{-1} respectively. The observed dependence of the rate of inactivation on the concentration of NADP$^+$ was used to estimate the apparent K_i for NADP$^+$ from a plot of the ratio of k in the presence of HNE to k_{app} in the presence of HNE and NADP$^+$ against the concentration of HNE. Although the rate of inactivation in the absence and the presence of NADP$^+$ was calculated by using different functions, the comparison of these calculated rates is valid because the Weibull function is only a generalization of the exponential function. The K_i(app) thus obtained is 41.7 ± 2.7 μM. For further kinetic characterization of HNE inactivation the reduced AR was modified by HNE until 50% of the enzyme activity was lost.

Partial modification of the enzyme by HNE (100 μM) led to a 17-fold increase in $K^{\mathrm{HNE}}{}_{\mathrm{m}}$ and $K^{\mathrm{glyceraldehyde}}{}_{\mathrm{m}}$, and a 3-fold increase in $K^{\mathrm{NADPH}}{}_{\mathrm{m}}$, whereas the k_{cat} with glyceraldehyde/NADPH and HNE/NADPH of the HNE-modified enzyme were decreased by 55% and 30%, respectively (Table 2). The changes in K_m and k_{cat} of the HNE-modified enzyme were similar to the changes caused by carboxymethylation of the enzyme (Table 2). The carboxymethylated enzyme was not inactivated by HNE; the carboxymethylated enzyme and the HNE-modified enzyme were relatively insensitive to sorbinil. The IC_{50} of sorbinil increased from 2 μM for the reduced enzyme to 1.04 mM for the carboxymethylated enzyme and 1.0 mM for the HNE-modified enzyme. The corresponding changes in K_i for tolrestat were smaller. The K_i for tolrestat was 0.04 μM for the reduced enzyme, which increased to 0.1 and 1.0 μM on carboxymethylation and HNE modification respectively.

Identification of HNE-modified residues

To identify the structural alterations leading to the inactivation, the enzyme was incubated with radiolabelled HNE. After 24 h of incubation at 4 °C, 2 mol of HNE were incorporated per mol of enzyme. The radiolabelled enzyme was digested with trypsin as described in the Materials and methods section. When the tryptic digest of the HNE-labelled enzyme was subjected to HPLC with an ODS C_{18} column, multiple peptide peaks were observed (Figure 4). Of these, three peaks contained significant radioactivity (marked A, B and C in Figure 4); they were purified, separated by HPLC, collected and sequenced with a gas-phase sequencer. The amino acid sequence (numbered in accordance to the human placental enzyme) of peptide A corresponded to Ile-260 to Cys-298, that of peptide B to Tyr-178 to Lys-195, and that of peptide C to Tyr-178 to Cys-187. These sequences showed a high degree of similarity to the analogous sequences of AR isolated from different tissues (Figure 5). However, few significant differences were noted. Like the bovine lens enzyme the bovine cardiac enzyme has a glutamine residue at position 275 in place of the Lys-275 present in placental AR. Moreover, residues

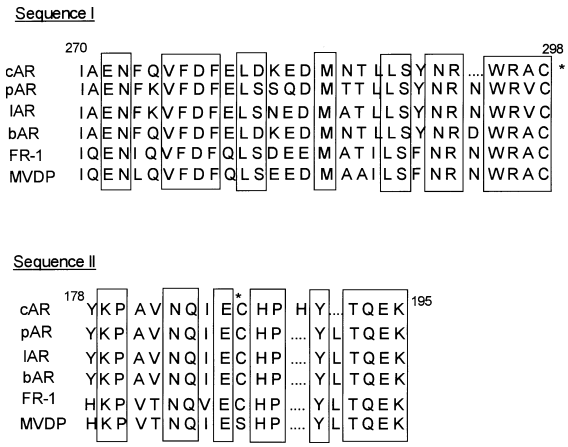

Figure 5 Alignment of amino acid sequences I and II of the cardiac AR (cAR) with equivalent sequences of AR from human placenta (pAR) [29], rat lens (lAR) [43], bovine lens (bAR) [44], FR-1 [31] and mouse vas deferens protein (MVDP) [30]

Amino acid sequences are aligned and the conserved residues are boxed. The radiolabelled cysteines are marked with an asterisk. The procedure for isolation of the two peptides is given in the text.

283–285 and 287–289 were not conserved between the AR forms from different tissues.

DISCUSSION

The results of this study show that the only significant pyridine coenzyme-linked oxidation/reduction of HNE in heart is associated with the polyol pathway enzyme AR. In other tissues several other oxidoreductases have been implicated in the metabolism and biotransformation of HNE and related α, β unsaturated aldehydes. For example, isoenzymes I and II of hepatic alcohol dehydrogenase catalyse HNE reduction with K_m values of 250–1430 μM and 100 μM respectively [15]. In the heart, isoenzyme III of alcohol dehydrogenase is the main enzyme, which displays a low affinity for HNE (K_m 6 mM) [16], and seems not to participate in HNE reduction. The NAD-dependent aldehyde dehydrogenase is another oxidoreductase suggested to catalyse HNE oxidation [2]. However, no significant aldehyde dehydrogenase activity was detected in the cytosolic fraction of the heart, consistent with earlier reports [17].

Although pulmonary carbonyl reductase oxidizes HNE with a K_m of 60 μM [18], it is a poor catalyst of HNE reduction (K_m = 6 mM). In view of the low activity of aldehyde oxidase in the myocardium, the contribution of $NADP^+$(H)-dependent carbonyl reductase is expected to be minimal. In agreement with this view, no significant NADP-dependent oxidation of HNE was observed in crude homogenates of mammalian hearts from any of the species examined (Table 1).

In non-muscle tissues, NADPH-dependent aldehyde reductase might represent another source of HNE metabolism [19,20]. Most non-muscle tissues examined in our laboratory show two NADPH-dependent aldehyde reductases, i.e. AR and aldehyde reductase, although aldehyde reductase activity in homogenates of aorta or skeletal muscle is immeasurably small [21]. However, no significant aldehyde reductase activity was observed on partial purification of bovine heart homogenates by DE-52 column chromatography. In agreement with our finding, Van der Jagt et al. [22] also failed to observe significant aldehyde reductase activity in heart. Thus, in the absence of a significant contribution of other oxidoreductases, AR seems to be the major myocardial pyridine-linked enzyme capable of utilizing HNE.

The affinity of AR for HNE ($K^{HNE}_m = 7$ μM) is higher than that of any other known enzyme capable of utilizing HNE. Hepatic aldehyde and alcohol dehydrogenases metabolize HNE with K_m values between 50 and 100 μM (see above), whereas the K^{HNE}_m of even the 'HNE-specific' glutathione S-transferase [23] is also between 50 and 100 μM [7,24]. The K_m of the cardiac AR for HNE is lower than those of other synthetic or natural substrates of this enzyme, but is comparable to that observed for other unsaturated aldehydes such as acrolein and methylglyoxal [25].

Catalytic competence of AR

For AR to be a competent catalyst of HNE reduction, it is essential for the enzyme to display a high affinity for this aldehyde and not be inactivated during catalysis. HNE avidly reacts with thiols [2] and could potentially inactivate AR, which contains a highly reactive thiol group (Cys-298) at the active site and is very sensitive to oxidation [14]. Our results show no substrate inhibition/inactivation of the enzyme during catalytic reduction of HNE, suggesting that the catalysis of HNE reduction by AR is not likely to be self-limiting. Nevertheless incubation of the apoenzyme with HNE did inactivate the enzyme. This seems to be due to a selective modification of the active site as well as non-specific oxidation of non-active-site thiol(s). Because HNE is a substrate of AR, it is expected that it will bind to the active site and, in the absence of catalysis, will react with Cys-298. Inactivation of the enzyme by HNE was rapid but was prevented by $NADP^+$. Given the very tight binding of the enzyme to $NADP^+$(H), most (approx. 95%) [26] of the enzyme under steady-state conditions is likely to be tied up in binary complexes and therefore insensitive to HNE. Thus HNE reduction by AR is unlikely to be inhibited by thiol modifications, unless of course HNE concentration reaches or exceeds cytotoxic levels (more than 100 μM).

The relevance of AR to HNE metabolism is further substantiated by the observation that the enzyme does not catalyse the oxidation of the alcohol (DHN) formed. The primary behaviour of the enzyme as an aldehyde reductase, and not an alcohol dehydrogenase, eliminates the possibility of futile cycling and/or inactivation due to the potentially suicidal behaviour of DHN.

Structural characteristics of cardiac AR

In its active form AR is a monomer and belongs to the β/α-barrel class of enzymes [27,28]. It displays high sequence similarity with aldehyde reductase [29], mouse vas deferens protein [30], the fibroblast growth factor inducible protein 1 (FR-1) [31] and the β subunit of the Shaker K^+ channel [32,33]. The HNE-reducing cardiac enzyme has structural and kinetic properties similar to those of AR purified from other tissues, particularly with regard to thiol modification. Modification of the cardiac enzyme with IAA led to an increase in the K_m of the enzyme for aldehyde substrates and a decrease in the sensitivity of the enzyme to sorbinil. Similar changes have been observed on carboxymethylation of the enzyme isolated from human placenta [34] or bovine lens [35].

Inactivation of the cardiac AR by HNE seems to be due to the modification of Cys-298, because modification of Cys-298 [36] of placental AR, and/or replacement of Cys-298 with a serine residue by site-directed mutagenesis [37] of recombinant AR, leads to changes similar to those observed with the HNE-

modified cardiac enzyme. This is substantiated by sequence analysis, which shows that Cys-298 and Cys-187 are modified by incubating the apoenzyme with HNE. Because Cys-298 is present at the active site, modification of this residue in the absence of $NADP^+(H)$ is expected and would lead to the observed changes in the kinetic properties of the enzyme. The role of Cys-187 in mediating HNE-induced changes is less clear. In placental AR, Cys-187 is present on the loop between β-strand S8 and the α-helix H6, which forms the wall of the barrel [38]. This residue is not exposed to the solvent and is located in the hydrophobic part of the protein. Modification of this residue by HNE is consistent with the high hydrophobicity of the aldehyde [39]. However, it is unlikely that modification of Cys-187 is responsible for enzyme inactivation, because AR carboxymethylated at residue 298 was insensitive to HNE. Moreover we found that AR in which Cys-298 had been replaced by serine was not inactivated by HNE (S. Srivastava, A. Chandra, A. Bhatnagar and S. K. Srivastava, unpublished work), indicating that inactivation of AR by HNE is primarily due to modification of Cys-298. For the same reasons it also seems unlikely that the inactivation of AR by HNE is due to lysine residues.

The amino acid sequences of the HNE-modified peptide of the cardiac AR show a striking similarity to equivalent sequences of AR isolated from other tissues. Although significant similarity was observed with other proteins (Figure 5), the HNE-reducing enzyme of the myocardium seems to be AR and not the structurally related proteins FR-1 or the mouse vas deferens protein MVDP.

In conclusion, the results of this study demonstrate that the main oxidoreductase associated with redox transformation of HNE in the myocardium is the polyol pathway enzyme AR. The enzyme displays an affinity for HNE higher than that reported for any other HNE-utilizing enzyme so far identified. The enzyme does not, however, catalyse alcohol oxidation and is therefore unlikely to be limited by product inhibition and/or inactivation. Although HNE inactivates the apoenzyme by covalent modification of thiols, the enzyme was insensitive to HNE during catalysis, presumably owing to the tight binding of the coenzyme. Partial sequence analysis suggests that the active site of the cardiac enzyme (like that of AR from other tissues) is well adapted to catalyse the reduction of hydrophobic aldehydes such as HNE, and corroborates the identification of the HNE-reducing enzyme as AR.

On the basis of these results we speculate that AR might represent an important component of cardiovascular antioxidative defences. Because α,β-unsaturated aldehydes, in addition to being products of endogenous lipid peroxidation, are present in several food substances and environmental pollutants and are generated during the metabolism of several drugs such as cyclophosphamide, and metabolites such as polyamines [2,40,41], a general role of AR in enal metabolism of the heart is indicated. This view is consistent with the increase in the expression of AR in vascular smooth-muscle cells exposed to HNE and H_2O_2 and the observed exacerbation of HNE toxicity by inhibitors of AR [42].

This study was supported in part by National Institutes of Health grants HL55477 and DK 36118.

REFERENCES

1 Lander, H. M. (1997) FASEB J. **11**, 118–124
2 Esterbauer, H., Schaur, R. J. and Zollner, H. (1991) Free Radicals Biol. Med. **11**, 81–128
3 Blasig, I. E., Grune, T., Schinheit, K., Rohde, E., Jakstadt, M. A., Haseloff, R. F. and Siems, W. G. (1995) Am. J. Physiol. **269**, H14–H22
4 Quinlan, G. J., Mumby, S., Pepper, J. and Gutteridge, J. M. C. (1994) Biochem. Mol. Biol. Internat. **34**, 1277–1282
5 Ollinger, K. and Brunmark, A. (1994) Biochem. Pharmacol. **48**, 1707–1715
6 Ishikawa, T., Esterbauer, H. and Sies, H. (1986) J. Biol. Chem. **261**, 1576–1586
7 Parinandi, N. L., Thompson, E. W. and Schmid, H. O. (1990) Biochim. Biophys. Acta **1047**, 63–69
8 Benedetti, A., Comporti, M. and Esterbauer, H. (1980) Biochim. Biophys. Acta **620**, 281–286
9 Bhatnagar, A. (1995) Circ. Res. **76**, 293–304
10 Chandra, A. and Srivastava, S. K. (1997) Lipids **32**, 779–782
11 Towbin, H., Staehelin, T. and Gordon, J. (1979) Proc. Natl. Acad. Sci. U.S.A. **76**, 4350–4354
12 Srivastava, S. K., Ansari, N. H., Hair, G. A. and Das, B. (1984) Biochim. Biophys. Acta **800**, 200–227
13 Cho, Y.-K. and Cook, P. F. (1988) J. Biol. Chem. **163**, 5135–5140
14 Bhatnagar, A. and Srivastava, S. K. (1992) Biochem. Med. Metabol. Biol. **48**, 91–121
15 Seelin, S., Holmquist, B., Mannervik, B. and Vallee, B. L. (1991) Biochemistry **30**, 2514–2518
16 Strydom, D. J. and Vallee, B. L. (1982) Anal. Biochem. **123**, 422–429
17 Manthey, C. L. and Sladek, N. E. (1989) Prog. Clin. Biol. Res. **290**, 49–63
18 Matsuura, K., Naganeo, F., Hara, A., Nakayama, T., Nakagawa, T. and Swada, H. (1989) Prog. Clin. Biol. Res. **290**, 335–349
19 Siems, W. G., Zollner, H. and Esterbauer, H. (1994) Cancer Res. **54**, 5231–5235
20 Kristal, B. S., Park, B. J. and Yu, B. P. (1994) Carcinogenesis **15**, 1359–1364
21 Srivastava, S. K., Ansari, N. H., Hair, G. A. and Das, B. (1984) Biochim. Biophys. Acta **800**, 220–227
22 Van der Jagt, D. L., Robinson, B., Taylor, K. K. and Hunsaker, L. A. (1990) J. Biol. Chem. **265**, 20982–20987
23 Stenberg, G., Ridderstrom, M., Engstrom, A., Pemble, S. E. and Mannervik, B. (1992) Biochem. J. **284**, 313–319
24 Singhal, S. S., Zimniak, P., Awasthi, S., Piper, J. T., He, N.-G., Tang, J. I., Peterson, D. R. and Awasthi, Y. C. (1994) Arch. Biochem. Biophys. **311**, 242–250
25 Van der Jagt, D. L., Kolb, N. S., Van der Jagt, T. J., Chino, J., Martinez, F. J., Hunsaker, L. A. and Royer, R. E. (1995) Biochim. Biophys. Acta **1249**, 117–126
26 Grimshaw, C. E., Bohren, K. M., Lai, C.-J. and Gabbay, K. H. (1995) Biochemistry **34**, 14366–14373
27 Rondeau, J. M., Tete-Favier, F., Podjarny, A., Reymann, J. M., Barth, P., Biellman, J. F. and Moras, D. (1989) Nature (London) **355**, 2912–2919
28 Wilson, D. K., Bohren, K. M., Gabbay, K. H. and Quiocho, F. A. (1992) Science **257**, 81–84
29 Bohren, K. M., Bullock, B., Wermuth, B. and Gabbay, K. H. (1989) J. Biol. Chem. **264**, 9547–9551
30 Pailhoux, E. A., Martinez, A., Veyssiere, G. M. and Jan, C. G. (1990) J. Biol. Chem. **265**, 19932–19936
31 Donohue, P. J., Alberts, G. F., Hampton, B. S. and Winkles, J. A. (1994) J. Biol. Chem. **269**, 8604–8609
32 McCormack, T. and McCormack, K. (1994) Cell **79**, 1133–1135
33 Chouinard, S. W., Wilson, G. F., Schilmgen, A. K. and Ganetzky, B. (1995) Proc. Natl. Acad. Sci. U.S.A. **92**, 6763–6767
34 Bhatnagar, A., Liu, S.-Q., Ueno, N., Chakrabarti, B. and Srivastava, S. K. (1994) Biochim. Biophys. Acta **1205**, 207–214
35 Liu, S.-Q., Bhatnagar, A. and Srivastava, S. K. (1992) Biochim. Biophys. Acta **1120**, 329–336
36 Liu, S.-Q., Bhatnagar, A., Ansari, N. H. and Srivastava, S. K. (1993) Biochim. Biophys. Acta **1164**, 268–272
37 Petrash, J. M., Harter, T. M., Devine, C. S., Olins, P. O., Bhatnagar, A., Liu, S.-Q. and Srivastava, S. K. (1992) J. Biol. Chem. **267**, 24833–24840
38 Harrison, D. H., Bohren, K. M., Ringe, D., Petsko, G. A. and Gabby, K. H. (1994) Biochemistry **33**, 2011–2020
39 Esterbauer, H. and Weger, W. (1967) Montash Chem. **98**, 1994–2000
40 Feron, V. J., Til, H. P., de Vrijer, F., Woutersen, R. A., Cassee, F. R. and van Bladeren, P. J. (1991) Mutat. Res. **259**, 363–385
41 Ghilarducci, D. P. and Tjeerdema, R. S. (1995) Rev. Environ. Contamin. Toxicol. **144**, 95–147
42 Spycher, S. E., Tabataba-Vakili, S., O'Donnell, V. B., Palomba, L. and Azzi, A. (1997) FASEB J. **11**, 181–188
43 Schade, S. Z., Early, S. L., Williams, T. R., Kezdy, F. J., Heinrikson, R. L., Grimshaw, C. E. and Doughty, C. C. (1990) J. Biol. Chem. **265**, 3628–3635
44 Petrash, J. M. and Favello, A. D. (1989) Curr. Eye Res. **8**, 1021–1027

Received 12 May 1997/28 August 1997; accepted 15 September 1997